Separation and Purification Technology 376 (2025) 133840

Contents lists available at ScienceDirect

Separation and Purification Technology

journal homepage: www.elsevier.com/locate/seppur

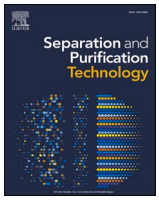

Separation of volatile fatty acids (VFAs) from nutrients in food waste using membrane contactor: Analysis of VFA-membrane interactions, separation efficiency, and nutrient rejection

Francis Kotoka [a,b,*], Leonardo Gutierrez [a,b,c], Emile Cornelissen [a,b,d]

[a] Particle and Interfacial Technology Group, Ghent University, Belgium
[b] Centre for Advanced Process Technology for Urban Resource Recovery (CAPTURE), Belgium
[c] Facultad del Mar y Medio Ambiente, Universidad del Pacifico, Ecuador
[d] KWR Water Research Institute, the Netherlands

ARTICLE INFO

Editor: Gaohong He

Keywords:
Fermentation
Surface free energy
Volatile fatty acids
Food waste
Hydrophobic membrane contactor

ABSTRACT

Membrane surface properties and interactions with organic species can influence selective separation processes such as hydrophobic membrane contactors (HMC). The selective separation of volatile fatty acids (VFAs) from nutrients in industrial fermented food waste (FFW) was investigated using HMC. The focus was on (1) interactions induced by VFAs on membrane surface, (2) trends in membrane surface free energy (Υ_S^{tot}), and (3) nutrient rejection (R_{Nut}) and VFA separation efficiency (S_{eff}). The Υ_S^{tot} and interactions varied with feed composition and concentration. The presence of VFAs increased the dispersive and polar interactions, and Lewis base components of the membrane surface by up to 2, 27, and 7-fold, respectively, while the Lewis acid components increased by three orders of magnitude. Consequently, the Υ_S^{tot} tripled at maximum compared to the Control membrane, leading to decreased R_{Nut} and VFA S_{eff}. The HMC separated 40–73 % of VFAs to the permeate while rejecting >95 % of nutrients in the feed. Increasing Υ_S^{tot} above 36 mJ/m^2 combined with decreasing water contact angle (WCA) below 90° were most detrimental to VFA S_{eff} and R_{Nut}.

1. Introduction

The presence of organic fractions in discharged waste streams causes economic losses and significant environmental damage, including high chemical oxygen demand (COD) and eutrophication [1,2]. To mitigate environmental harm from organic waste streams, current research focuses on converting organic fractions into volatile fatty acids (VFAs) and nutrients through anaerobic digestion and fermentation [3–7], aiming that the VFAs can partly or entirely be used for industrial and commercial applications [8]. With market demand ranging from US$600 to US$4000 per ton [9], VFAs have substantial potential as chemical platforms in the chemical and pharmaceutical industries [10–14], while the nutrients can be used in bio-based fertilizers.

Food waste (FW) is a considerable source for producing VFAs and releasing nutrients. Food and green wastes comprise 44 % of the 2.01 billion tonnes of global municipal solid waste [15]. Moreover, 4–30 g/L and 0.02–14.7 g/L VFAs and nutrients have been measured in fermented food waste (FFW) respectively [3,4,16–22]. Despite the availability of food wastes for VFA and nutrient production, selectively separating VFAs from nutrients in FFW is challenging due to the complexity of the fermented media [3,4,16,17,21,22]. For this purpose, various membrane-based, adsorption–desorption, precipitation, extraction, and chromatographic methods have been explored [16,23–27]. These methods often face constraints like high energy consumption (thermally driven membrane distillation), low VFA-nutrient selectivity (electrodialysis), high operating pressure (RO and NF), or significant chemical usage (chemical extraction) [16,23].

Among these methods, direct contact hydrophobic membrane contactor (HMC) and adsorption–desorption have gained attention due to their higher affinity for VFAs over nutrients [8,24,27–30]. Briefly, 76 kg VFAs per kg adsorbent or 68–89 % VFAs were separated from model and real VFA solutions using adsorption–desorption [30–32]. However, in some cases, adsorbents suffer from co-adsorption of H_2SO_4, HCl, and H_3PO_4 [30]. In most cases, the desorption step requires high temperature (e.g., 120–200 °C) and high chemical addition [30–32]. Therefore, HMC is widely utilized for VFA separation from FFW due to its lower energy demand and reduced chemical additive requirements compared

* Corresponding author at: Particle and Interfacial Technology Group, Ghent University, Belgium.
E-mail address: francis.kotoka@ugent.be (F. Kotoka).

https://doi.org/10.1016/j.seppur.2025.133840
Received 25 January 2025; Received in revised form 14 April 2025; Accepted 1 June 2025
Available online 3 June 2025

Nomenclature

$[RCOO^-]$	Total molar amount of dissociated VFA in the feed
$[RCOOH]_p$	Total molar amount of protonated VFA in the feed
$[RCOOH_p + RCOO^-]_T$	Total molar amount of protonated and dissociated VFAs in the feed
B0 (i)	Feed solution containing 0.05 equimolar (Nutrients + C_2 + C_3 + C_4)
B0 (ii)	Feed solution containing 0.05 equimolar (Nutrients + C_5 + C_6 + C_8)
B0 (iii)	Feed solution containing 0.05 equimolar (Nutrients + C_2 + C_3 + C_4 + C_5 + C_6 + C_8)
B1 (ii)	Feed solution containing 0.0075 M C_5 + 0.0075 M C_6 + 0.0035 M C_8 + 0.05 M Nutrients
B1 (iii)	Feed solution containing 0.05 equimolar (C_2 + C_3 + C_4) + 0.0075 M C_5 + 0.0075 M C_6 + 0.0035 M C_8 + 0.05 M Nutrients
B2	Feed solution containing 0.035 M C_2 + 0.01 M C_3 + 0.035 M C_4 + 0.05 M Nutrients
C_2	Acetic acid
C_2-C_4	Combination of acetic, propionic and butyric acid
C_2-C_8	Combination of acetic, propionic, butyric, valeric, caproic, and caprylic acid
C_3	Propionic acid
C_4	Butyric acid
C_5	Valeric acid
C_5-C_8	Combination of valeric, caproic, and caprylic acid
C_6	Caproic acid
C_8	Caprylic acid
Control	Feed solution containing nutrients only (without VFAs)
DPM	Dry pristine membrane
FFW	Fermented food waste
FW	Food waste
N	Membrane exposed to Control feed solution
NC_2-C_4	Membrane exposed to feed solution containing (Nutrients + C_2 + C_3 + C_4)
NC_2-C_8	Membrane exposed to feed solution containing (Nutrients + C_2 + C_3 + C_4 + C_5 + C_6 + C_8)
NC_5-C_8	Membrane exposed to feed solution containing (Nutrients + C_5 + C_6 + C_8)
$n_{F,0}^{Nut}$	Initial amount (mol) of nutrients in feed solution
$n_{F,0}^{VFA}$	Initial amount (mol) of VFA in the feed
$n_{F,t}^{Nut}$	Amount (mol) of nutrients in feed solution at any given time
$n_{p,t}^{VFA}$	Amount (mol) of VFA in the permeate at any given time
P_{ow}	Octanol-water partition coefficient
RFFW	Membrane exposed to real feed solution (FFW)
R_{Nut}	Nutrient rejection
S_{eff}	Separation efficiency
WCA	Water contact angle
β	Percent protonated VFA (undissociated VFA) in the feed
θ	Liquid contact angle on membrane
Υ_{LV}	Liquid (water, or diiodomethane, or glycerol) surface tension
Υ_{LV}^-	Lewis base component of liquid surface
Υ_{LV}^+	Lewis acid component of liquid surface
Υ_{LV}^d	Dispersive component of liquid surface
Υ_{LV}^{LW}	Lifshitz Van der Waal component of liquid surface
Υ_{LV}^p	Polar component of liquid surface
Υ_S^-	Lewis base component of membrane surface
Υ_S^+	Lewis acid component of membrane surface
Υ_S^{AB}	Lewis acid-base component of membrane surface
Υ_S^d	Dispersive component of membrane surface
Υ_S^{LW}	Lifshitz Van der Waal component of membrane surface
Υ_S^p	Polar component of membrane surface
Υ_S^{tot}	Surface free energy of membrane surface

to adsorption–desorption [29,33,34]. For instance, 10–98 % VFAs have been separated from model and real streams using HMC [16,29,35,36].

Operating conditions substantially impact VFA recovery in HMC [37,38]. Briefly, increasing feed temperature by 10 °C from 25 °C enhanced the diffusion coefficient by 33 %, while a 3.2-fold increase in flow rate nearly doubled the VFA transport [37]. In addition to operating conditions, membrane materials like polyvinylidene fluoride (PVDF), polyethersulfone (PES), polytetrafluoroethylene (PTFE), silicone, polysulfone (PS), polyethylene (PE), and polypropylene (PP) have been employed for VFAs separation due to their high hydrophobicity, large interfacial area, and superior selectivity for VFAs over nutrients [29,35,39,40]. About 96–98 % VFAs were recovered using PTFE and PE membranes while rejecting 98–100 % nutrients [16,29].

Clearly, all the studies focused on operating conditions and membrane materials on separation efficiency (S_{eff}) of VFAs neglecting the membrane surface interactions induced by VFAs and their effects on VFA S_{eff} and nutrient rejection (R_{Nut}). The membrane surface free energy (Υ_S^{tot}) describes the equilibrium state of atoms on the membrane surface, influencing wetting, dispersion, dipole–dipole interactions, and Lewis-acid-base interactions [41,42]. Therefore, interactions between the VFAs and the membrane surface, and changes in Υ_S^{tot} during HMC may influence the membrane behavior and impact the VFA S_{eff} and nutrient rejection (R_{Nut}) [43,44]. To the best of our knowledge, this study is the first to investigate the membrane surface interactions and Υ_S^{tot} effect on R_{Nut} and VFA S_{eff} via PTFE HMC.

The objectives of this study are to investigate (1) surface interactions induced by VFAs on HMC membrane surface, (2) trend in membrane Υ_S^{tot} influenced by VFAs, and (3) R_{Nut} and VFA S_{eff} via PTFE HMC applied to FFW. For that purpose, HMC was applied to separate VFAs (acetic (C_2), propionic (C_3), butyric (C_4), valeric (C_5), caproic (C_6), and caprylic (C_8) acids) from synthetic solutions, and industrial FFW while rejecting nutrients. Thereafter, liquid (water, diiodomethane, and glycerol) contact angles on the membranes were measured to calculate the magnitude of VFA-membrane interactions. This study demonstrates how VFA-membrane interactions alter Υ_S^{tot} and water contact angle (WCA) which influence VFA S_{eff} and R_{Nut} in HMC. Particularly, it highlights the critical role of maintaining optimal WCA and Υ_S^{tot} in enhancing VFA S_{eff} and R_{Nut} during HMC applied to FFW. By demonstrating how these membrane surface properties directly influence separation performance, the findings offer a valuable pathway for improving the recovery and valorization of VFAs and nutrients. This not only supports the advancement of sustainable resource recovery and circular economy but also contributes to reducing adverse environmental impacts of food waste.

2. Materials and methods

2.1. Membranes, chemical reagents, and fermented food wastes

The PTFE membrane had a thickness of 230 μm, a pore size of 0.45 μm (provided by manufacturer), and a water contact angle (WCA) of 136.95 ± 3.59°. It was purchased from Aquastill BV (Nusterweg 69, the Netherlands). PTFE membrane was chosen because of its high hydrophobicity, and VFA selectivity against inorganic ions making it suitable for VFA recovery via HMC as widely reported in literature [29,37,38,45,46]. Additionally, PTFE has low Υ_S^{tot} (18–22 mJ/m^2), making it suitable for repelling water and minimizing potential organic fouling [47–51]. The acetic (96 % purity), propionic (99.5 %), butyric

(≥99 %), valeric (99 %), caproic (99 %), and caprylic (99 %) acids bought from Sigma-Aldrich (Belgium) were used as synthetic VFAs. The $KOH_{(s)}$ (≥99 %), $NH_4OH_{(l)}$ (≥25 %), $HNO_{3(conc)}$ (65 %), $H_3PO_{4(conc)}$ (≥85 %), $NaOH_{(s)}$ (≥98.5 %) and $HCl_{(conc)}$ (37 %) were purchased from Sigma-Aldrich (Belgium). The FFW prepared from fruits and vegetable wastes was obtained from Dranco nv (Belgium).

2.2. Nutrient rejection and VFA separation efficiency from synthetic feed

In this section, the feed solutions were categorized into four groups, namely Control, B0, B1, and B2 (Table 1). The B0 and B1 groups were further subdivided to account for variations in VFA and nutrient compositions. B0 was subdivided into B0 (i), B0 (ii), and B0 (iii), whereas B1 was subdivided into B1 (ii), and B1 (iii). The compositions of B0 (i), B0 (ii), B0 (iii), B1 (ii), and B1 (iii), and B2 are described in Table 1. The selection of C_2 to C_8 as feed VFAs was based on feed composition of FFW in this study and literature [18,19,22,38,39,52,53]. Normally, FFW is dominated by high molar concentration of C_2 to C_4 (C_2-C_4) [4,18,39,54,55], hence, equimolar and non-equimolar concentrations of C_2-C_4 were prepared in B0 (i), and B2 respectively. However, since the highest individual nutrient concentration was 0.05 M (Table 2), the maximum individual C_2-C_4 concentration was maintained at 0.05 M which was within the range of C_2-C_4 concentrations in FFW [4,18,38,39,54,55]. Equimolar concentration was necessary to equally compare the impacts of nutrients and C_2-C_4 on the membrane. Additionally, to compare the influence of C_2-C_4, and nutrients with C_5 to C_8 (C_5-C_8), similar equimolar concentrations of C_5-C_8 were also prepared as shown in B0 (ii). A combined equimolar mixture of C_2-C_8, based on concentrations from B0 (i) and B0 (ii) was prepared in B0 (iii) to evaluate the overall influence of VFAs. Feed solutions B1 (ii), B1(iii), and B2 were prepared to explore non-equimolar concentrations of VFAs. In FFW, individual C_5, C_6 and C_8 concentration range 130–2000 mg/L with typical total molar concentration of ~0.02 M has been reported [22,52,56], therefore B1 (ii) was prepared within the range, having total concentration of ~0.02 M. Typically, FFW is dominated by total molar concentration of C_2-C_4 as in B0 (ii) and less C_5-C_8 as in B1 (ii) [18,22,38,52], hence, B1 (iii) was prepared to contain VFAs dominated by C_2-C_4 concentration compared to C_5-C_8. Thus, VFA concentrations in B0 (i), and B1 (ii) were maintained in B1 (iii) to make a fair comparison. Given that the real feed has a pH of around 5, all experiments were conducted at a feed pH of 5.

Table 1
Overview of experiments using model feed solutions.

Component	Control	B0 (mol/L)	B1 (mol/L)	B2 (mol/L)
Nutrients (0.05 equimolar)	Mixed K^+ NO_3^- NH_4^+ $H_2PO_4^-$			
Nutrients + C_2-C_4		B0 (i): 0.05 equimolar (Nutrients + C_2 + C_3 + C_4)		B2: 0.035C_2 + 0.01C_3 + 0.035 C_4 + 0.05 Nutrients
Nutrients + C_5-C_8		B0 (ii): 0.05 equimolar (Nutrients + C_5 + C_6 + C_8)	B1 (ii): 0.0075 C_5 + 0.0075C_6 + 0.0035C_8 + 0.05 Nutrients	
Nutrients + C_2-C_8		B0 (iii): 0.05 equimolar (Nutrients + C_2 + C_3 + C_4 + C_5 + C_6 + C_8)	B1 (iii): 0.05 equimolar (C_2 + C_3 + C_4) + 0.0075 C_5 + 0.0075C_6 + 0.0035 C_8 + 0.05 Nutrients	

C_2-C4 represents a combination of acetic, propionic and butyric acid. C_5-C_8 represents a combination of valeric, caproic and caprylic acid. C_2-C_8 represents combination of acetic, propionic, butyric, valeric, caproic, and caprylic acid.

Table 2
VFA and nutrient content of FFW.

VFA	Concentration (mg/L)	Nutrients and other ions (mg/L)
Acetic acid: C_2	4308 ± 186	1881 ± 134 K^+
Propionic acid: C_3	401 ± 71	634 ± 88 NH_4^+
Butyric acid: C_4	1245 ± 84	225 ± 51 NO_3^-
Valeric acid: C_5	156 ± 59	409 ± 77 $H_2PO_4^-$
Caproic acid: C_6	1783 ± 111	296 ± 49 SO_4^{2-}
Caprylic acid: C_8	368 ± 97	1201 ± 88 Cl^-
Conductivity (11.5 mS/cm)		236 ± 41 Mg^{2+}
pH 5.01		621 ± 71 Ca^{2+}
		152 ± 32 Na^+

The Control solution (without VFAs), containing 0.05 equimolar of mixed K^+, NO_3^-, NH_4^+, and $H_2PO_4^-$ in a 1 L volumetric flask, was prepared using KOH, HNO_3, NH_4OH, and H_3PO_4. Individual K^+, and NH_4^+ concentrations in FFW (Table 2) were 0.04–0.05 M while NO_3^-, and $H_2PO_4^-$ were 0.004 M each. However, nutrient concentration in FFW is normally dominated by K^+, and NH_4^+ than $H_2PO_4^-$, and NO_3^- [4,16,57,58]. Therefore, to equally compare the impact of the nutrients and VFAs at the same concentration, the 0.05 M equimolar concentration was chosen and used as the Control. Thus utilizing 0.004 M equimolar of C_2-C_4 for example due to the 0.004 M NO_3^-, and $H_2PO_4^-$ would result in too low concentration of C_2-C_4 outside the range observed in literature [4,18,38,39,54,55]. Ca^{2+}, Mg^{2+}, and SO_4^{2-} nutrients were excluded from the synthetic solution to avoid precipitation with sulphate, phosphate, and the VFAs. Na+, and Cl^- were also excluded because they are not considered nutrients. A 0.1 N $NaOH_{(aq)}$ solution (pH 13) was prepared in a 2 L volumetric flask and used as the permeate solution [3,4,16,17,35,37–39,57]. To assess R_{Nut} in the absence of VFAs, 150 mL of each of the Control feed solution and permeate solution were transferred into the HMC feed and stripping chambers, separated by a 5.31 cm^2 membrane (Fig. 1) and stirred at 20 % using a LABINCO stirrer (model LD-746, The Netherlands). The experiment was conducted at 25 °C for 24 h. To investigate the VFA S_{eff} and R_{Nut}, 0.5 L of each feed solution was prepared by mixing nutrients with different concentrations of VFAs (Table 1). The experiment was repeated using 150 mL of each feed solution: B0 (i), B0 (ii), B0 (iii), B1 (ii), B1 (iii), and B2 separately. Throughout these experiments, we maintained consistent volumes for both feed and permeate solutions, as well as uniform pH levels, stirring rates, operation time, and temperature, which were identical to those used with the Control feed solution.

2.3. Nutrient rejection and VFA separation efficiency from FFW

The VFA S_{eff} and R_{Nut} from FFW were studied via HMC (Fig. 1). The FFW (Table 2) was filtered through a flat sheet commercial ceramic membrane (SiC) with a surface area of 0.17 m^2, a pore size of 0.56 μm, and a porosity of 42 % to remove suspended particles. The same operating conditions were maintained as in Section 2.2.

The concentrations of cations were determined using a Metrohm 930 Compact IC Flex ion chromatography machine (Switzerland) with a Metrosep C_6-150/4.0 column, while inorganic anions were quantified using Metrosep A Supp 16–250/4.0 column and Metrosep organic acids 250/7.8 column, respectively. VFA concentrations were measured using gas chromatography (GC-2010 Plus, Japan).

2.4. Membrane surface characterization via contact angle measurements

Each membrane used for VFA separation from nutrients (Tables 1 and 2) was removed from the HMC set-up (Fig. 1) after 24 h. The membranes were then vertically clamped in the air for 2 h to remove excess water from their surfaces. This approach was adopted to minimize water interference on the membrane surface during subsequent

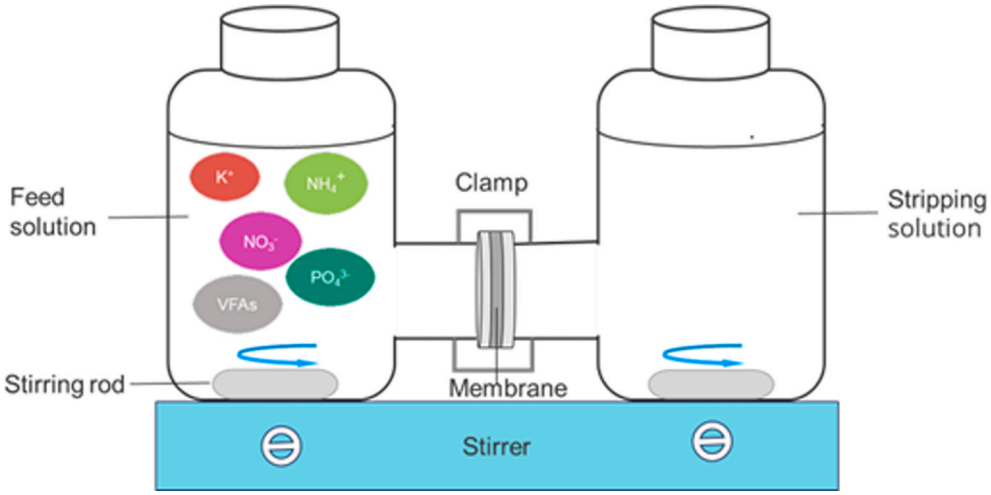

Fig. 1. Experimental set-up of HMC.

contact angle measurements. The resulting membranes were labeled as N, NC_2-C_4 and NC_5-C_8, NC_2-C_8, and RFFW, corresponding to membranes exposed to nutrients only (Control feed), Nutrients + C_2-C_4, Nutrients + C_5-C_8, Nutrients + C_2-C_8, and FFW respectively. Water contact angle (WCA) measurements were conducted using a goniometer (Krüss, DSA25, Germany) at 20 °C [59]. WCAs were determined at five positions on the membrane surface previously in contact with feed solutions. To assess surface interactions and Υ_S^{tot}, contact angle measurements were also performed using diiodomethane and glycerol [41,42,60]. All experiments in Sections 2.1 to 2.4 were performed in triplicate unless otherwise specified.

2.5. Separation efficiencies, surface interactions, and surface free energy calculations

The S_{eff} of VFA (Eq. (1)) describes the percentage of VFAs separated by the membrane.

$$S_{eff} = 100 \times \left(\frac{n_{p,t}^{VFA}}{n_{F,0}^{VFA}}\right) \quad (1)$$

Here, $n_{p,t}^{VFA}$ is the amount (mol) of VFA in the permeate at a given time, and $n_{F,0}^{VFA}$ is the initial quantity (mol) of VFAs in the feed solution.

The relation between the liquid contact angles, dispersive component (Υ_S^d), and polar component (Υ_S^p) of membrane surface is expressed by Eq. (2) [60,61]. The Υ_S^d and Υ_S^p were obtained using Eq. (3), as demonstrated in [41,42,47].

The Υ_S^d and Υ_S^p relate to the Lifshitz Van der Waal component (Υ_S^{LW}) described in (Eq. (4) [41,42,47].

$$\gamma_{LV} \times (1 + cos\theta) = 2 \times \left(\gamma_{LV}^d \times \gamma_S^d\right)^{0.5} + 2 \times \left(\gamma_{LV}^p \times \gamma_S^p\right)^{0.5} \quad (2)$$

Here θ, Υ_{LV}, Υ_{LV}^d, Υ_{LV}^p are the contact angle of the liquid (water, diiodomethane, or glycerol) on the surface of the membrane, surface tension, dispersive component, and polar component of the liquid surface.

$$\frac{0.5\gamma_{LV}(1 + cos\theta)}{\left(\gamma_{LV}^d\right)^{0.5}} = \left(\gamma_S^p\right)^{0.5}\left(\frac{\gamma_{LV}^p}{\gamma_{LV}^d}\right)^{0.5} + \left(\gamma_S^d\right)^{0.5} \quad (3)$$

$$\gamma_S^{LW} = \gamma_S^d + \gamma_S^p \quad (4)$$

The Lewis acid-base component (Υ_S^{AB}) demonstrates acidity (electron-pair acceptor interactions, Υ_S^+) and/or basicity (electron-pair donor interactions, Υ_S^-) of the membrane surface (Eqs. (5) and (6) [42,60].

$$0.5\gamma_{LV}(1 + cos\theta) = \left(\gamma_{LV}^{LW}\right)^{0.5}\left(\gamma_S^{LW}\right)^{0.5} + \left(\gamma_{LV}^+\right)^{0.5}\left(\gamma_S^-\right)^{0.5} + \left(\gamma_{LV}^-\right)^{0.5}\left(\gamma_S^+\right)^{0.5} \quad (5)$$

$$\gamma_S^{AB} = 2 \times \left(\gamma_S^+ \times \gamma_S^-\right)^{0.5} \quad (6)$$

Here γ_{LV}, γ_{LV}^{LW}, γ_{LV}^+, and γ_{LV}^- sequentially represent the surface tension, Lifshitz Van der Waal, electron-pair acceptor (Lewis acid), and electron-pair donor (Lewis base) components of liquid (either water, diiodomethane, or glycerol. The γ_S^+, and γ_S^- represent the electron-pair acceptor (Lewis acid component) and electron-pair donor (Lewis base component) of the membrane surface. The γ_{LV}^+ and γ_{LV}^- were considered zero for diiodomethane, as reported elsewhere [42,49,60].

The Υ_S^{tot}, which encompasses overall intermolecular forces and acid-base components of membrane surface, was calculated using Eq. (7) [41,42,60,61].

$$\gamma_S^{tot} = \gamma_S^{LW} + \gamma_S^{AB} \quad (7)$$

The nutrient rejection (R_{Nut}) was calculated using Eq. (8).

$$R_{Nut}(\%) = 100 \times \left(\frac{n_{F,t}^{Nut}}{n_{F,0}^{Nut}}\right) \quad (8)$$

$n_{F,t}^{Nut}$ is the amount (mol) of nutrients in the feed at a given time, and $n_{F,0}^{Nut}$ is the initial quantity (mol) of nutrients in the feed solution. The percent of protonated VFAs in the feed was calculated from Eq. (9) [16,37].

$$\beta = \frac{[\mathrm{RCOOH}]_p}{\left[\mathrm{RCOOH}_p + \mathrm{RCOO}^-\right]_T} \times 100 = \left(\frac{10^{(pKa-pH)}}{1 + 10^{(pKa-pH)}}\right) \times 100 \quad (9)$$

where β is percent protonated VFA (undissociated VFA) in the feed, $[\mathrm{RCOOH}]_p$ is total molar amount of protonated VFA in the feed, $[\mathrm{RCOO}^-]$ is total molar amount of dissociated VFA (unprotonated) in the feed, and $\left[\mathrm{RCOOH}_p + \mathrm{RCOO}^-\right]_T$ is the total molar amount of protonated and dissociated VFAs in the feed.

3. Results and discussion

3.1. Water, diiodomethane, and glycerol contact angles on the membrane

The liquid contact angles were initially measured on the dry pristine membrane (DPM) and subsequently on membranes exposed to various feed solutions. The DPM exhibited a high WCA of 137 ± 4° prior to experimentation. Post-experimentation, the WCAs of membranes exposed to the various feed decreased by 1.1–3.3-fold compared to the DPM (Fig. 2a). Despite the decrease in WCA, each membrane exposed to

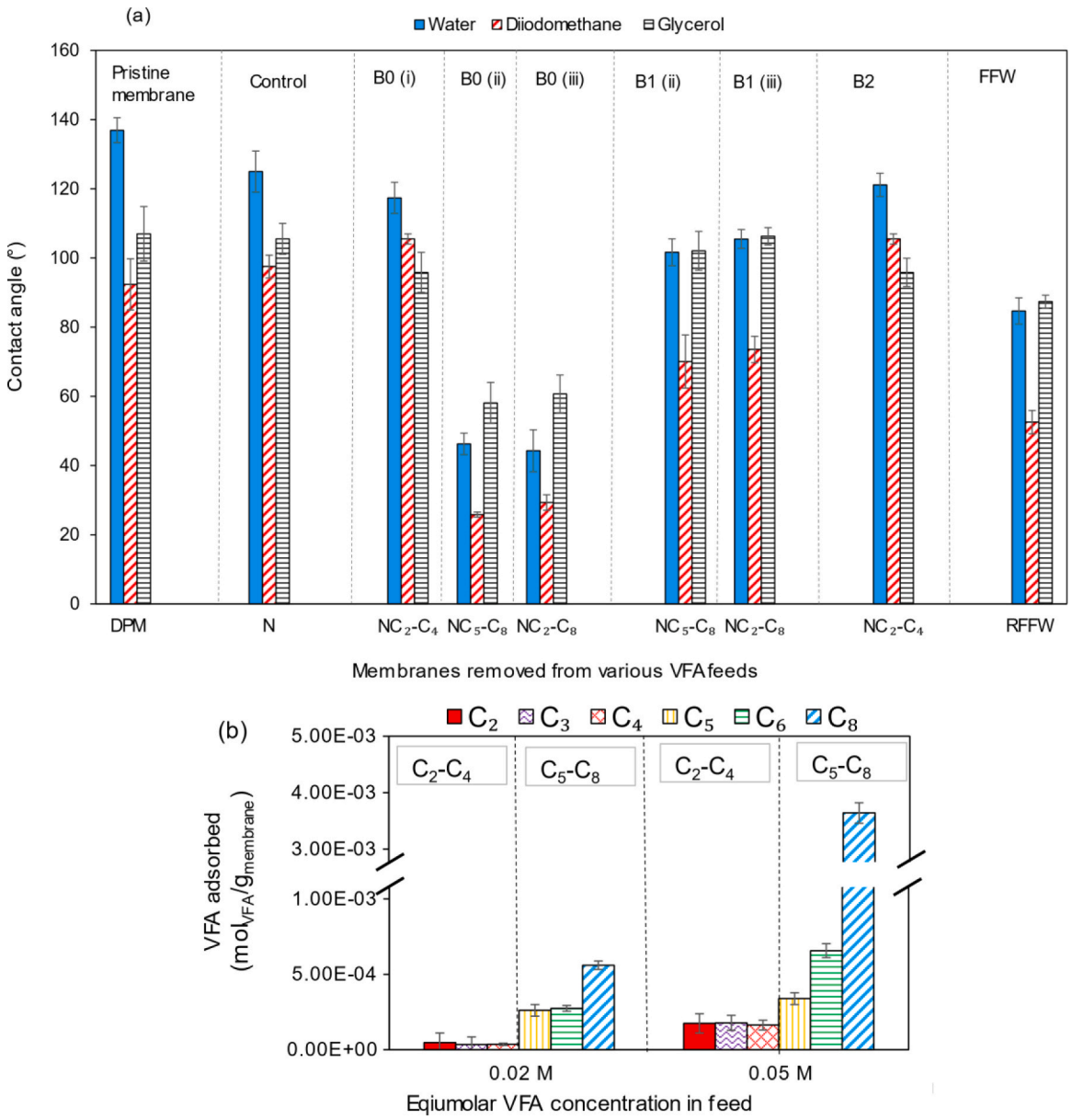

Fig. 2. (a) Liquid contact angles of membranes; (b) VFA adsorbed by membrane. The N, NC_2-C_4, NC_5-C_8, NC_2-C_8, and RFFW denote membranes exposed to nutrient feed only (Control), nutrients mixed with C_2-C_4, nutrients mixed with C_5-C_8, nutrients mixed with C_2-C_8, and FFW respectively (refer to Tables 1 and 2).

the Control, B0 (i), B1 (ii), B1(iii), and B2 maintained WCA above 90°. A WCA >90° suggests that the membranes retained some level of hydrophobicity during HMC operation. Nonetheless, the WCA of NC_5-C_8 and NC_2-C_8 membranes removed from B0 (ii) and B0 (iii) decreased below 90°. The decreased WCA was particularly noticeable in membranes exposed to high concentrations of C_5-C_8 compared to C_2-C_4 (Fig. 2a).

A follow-up adsorption experiment was conducted by introducing 150 mL each of the B0 feed containing equimolar VFAs into the feed and permeate chambers of Fig. 1. The C_5-C_8 adsorbed within 24 h were 9-fold the C_2-C_4. (Fig. 2b). Particularly, C_8 and C_6 were the most adsorbed VFAs. A previous study demonstrated that fatty compounds, e.g C_5-C_8, act as surfactants by adsorbing at the solid–liquid interface, leading to decreased WCAs [62,63]. WCA below 90° is very detrimental to VFA S_{eff}, and R_{Nut} since salts and inorganic ions rapidly penetrate the membrane [43,44,64–66], competing with the VFAs.

3.2. Lifshitz Van der Waal, polar, dispersive components on membrane

The DPM exhibited Van der Waal (γ_S^{LW}), dispersive (γ_S^d), and polar (γ_S^p) components of 14.1, 13.1, and 0.96 mJ/m^2, respectively (Fig. 3a). These values align with literature reports ranging from 14 to 15.7 mJ/m^2 for γ_S^{LW}, 15.1 mJ/m^2 for γ_S^d, and 0.1–1.5 mJ/m^2 for γ_S^p [47–49]. Across all membranes tested, γ_S^d dominated the membrane surfaces compared to γ_S^p, contributing to 64–98 % and 2–36 % of γ_S^{LW}, respectively (Fig. 3a and b). Higher γ_S^d and γ_S^p values were observed on the membranes exposed to the B0 feeds, containing the highest VFA concentration, while lower values were noted in B2 and B1 due to lower VFA concentrations. Since HMC is a diffusion process, increasing VFA concentration promotes high VFA flux [29,37,39], and increases VFA-membrane interactions. This accounts for the maximum γ_S^d and γ_S^p of membranes exposed to all B0 feed solutions but minimum in B2 and B1. However, increasing VFA concentration can cause excessive VFA adsorption on membrane surface, and decrease WCA (Fig. 2a, and b), leading to decreased R_{Nut}.

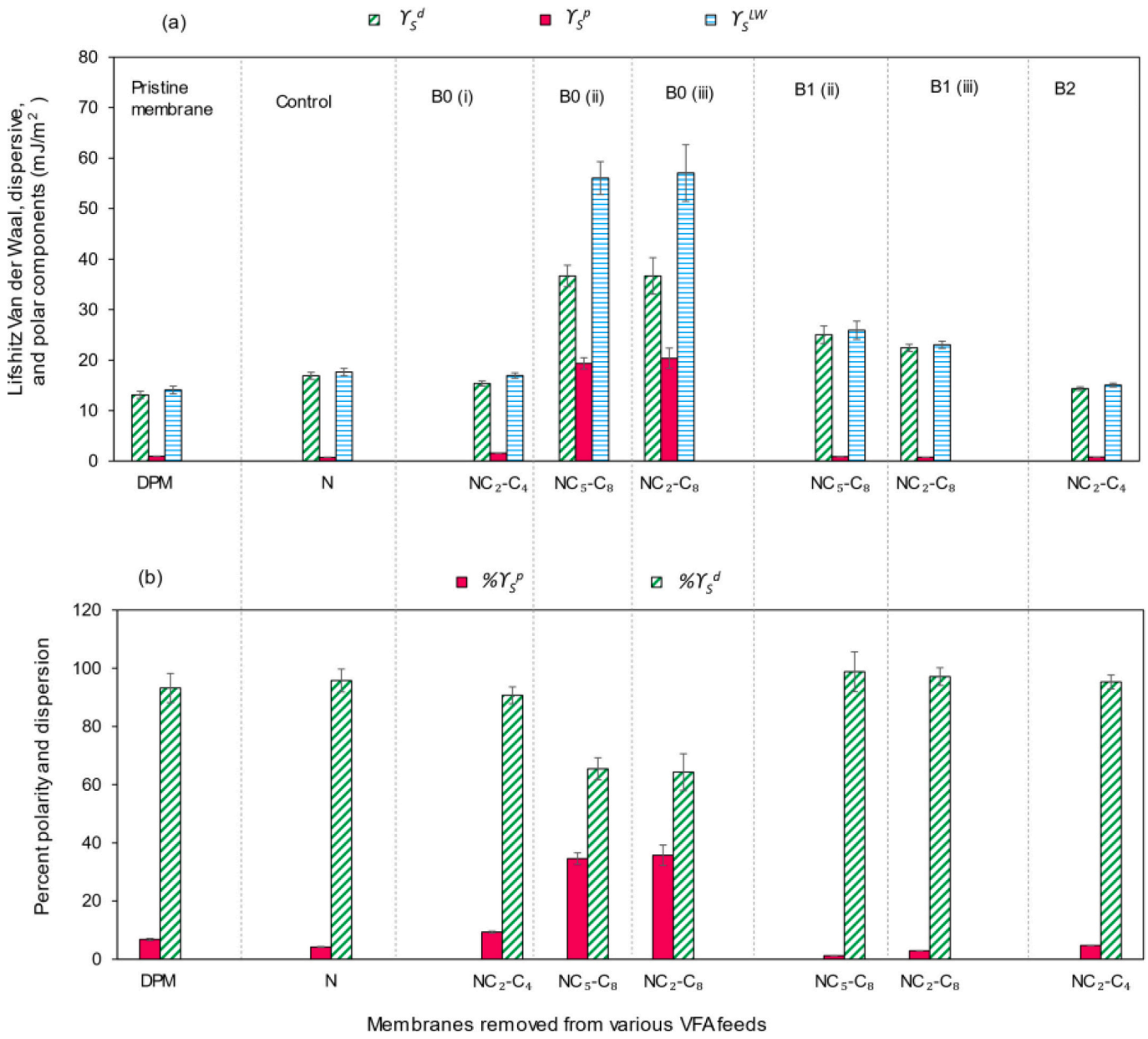

Fig. 3. (a) Lifshitz Van der Waal components; (b) percent polarity, and dispersion on PTFE membrane surface (refer to Tables 1 and 2 for compositions of N, B0 (i), B0 (ii), B0 (iii), B1(ii), B1(iii), and B2).

Dispersive interactions are ubiquitous and operate even at molecular and atomic scales [67]. The VFAs contain multiple atoms. Therefore, the transfer of VFAs onto the membrane increased atomic and molecular interactions, thereby amplifying γ_S^d (Fig. 3a). The increased γ_S^d caused by VFAs suggests a higher affinity of the membrane for VFAs over the nutrients [29], which is desirable for high VFA S_{eff} and R_{Nut}. Similarly, due to the polarity of –COOH group [59–62]; the VFAs on the membrane reinforced γ_S^p. Nonetheless, since some nutrients, protonated, and dissociated VFAs in the feed have comparable polarities, it is insufficient to attribute the change in polarity solely to the –COOH without considering Lewis acid (γ_S^+) and Lewis base (γ_S^-) components yet to be discussed in Section 3.4.

The influence of C_5-C_8 on surface interactions was pronounced compared to equimolar amounts of C_2-C_4. For example, the NC_5-C_8 membrane from B0 (Table 1) displayed γ_S^d, γ_S^p and γ_S^{LW} 2.5 and 12.2, and 3-fold the values exhibited by NC_2-C_4, respectively (Fig. 3a). Due to the higher hydrophobicity of C_5-C_8, they exhibit a stronger affinity towards hydrophobic membranes [29,35,37] than C_2-C_4. Moreover, C_5-C_8 contains more atoms, which enhances dispersive interactions than C_2-C_4. The increased γ_S^d and γ_S^p caused by NC_5-C_8 compared to NC_2-C_4 indicate that γ_S^{LW} of NC_2-C_8 was primarily contributed by C_5-C_8. The higher γ_S^d and γ_S^p induced by the C_5-C_8 imply that the membrane has superior affinity for C_5-C_8, hence higher flux and S_{eff} compared to C_2-C_4. A previous study demonstrated that the PTFE membrane exhibited higher mass transfer coefficients for C_6 and C_8, which were 1.1 to 4.4-fold the values attained for C_2, C_3, and C_4 [35].

For non-equimolar concentrations, decreasing the VFA concentration decreased the γ_S^d and γ_S^p due to a lower amount of atoms interacting with the membrane. Thus, decreasing C_2-C_4, C_5-C_8, and C_2-C_8 concentrations in B0 (i), B0 (ii), and B0 (iii) feed respectively to the concentrations of B2, B1 (ii), and B1 (iii) reduced the magnitude of γ_S^d and γ_S^p on the NC_2-C_4, NC_5-C_8, and NC_2-C_8 membranes (Fig. 3a).

3.3. Proposed mechanisms of surface characteristics and effect on R_{Nut} and VFA S_{eff}

VFAs decrease WCA and increase membrane surface interactions through two main mechanisms. Firstly, VFAs accumulate on the feed water surface [68–71]. As surfactants, VFAs accumulate on water surface and within water molecules due to their hydrophobic alkyl carbon chains (Fig. 4). This disrupts cohesive forces between water molecules, leading to rapid water spreading and decreasing WCA. In the absence of VFAs (Fig. 4a), or at low VFA concentrations (Fig. 4b), compared to high VFA concentration (Fig. 4c), surface accumulation of VFAs is minimized, hence less membrane wetting occurs, leading to high VFA S_{eff} and R_{Nut}.

Secondly, VFAs adsorb at the feed-membrane interface (Fig. 4b, and c), leading to a decreased interfacial tension [72]. The VFAs adsorb mainly via dispersive (Fig. 3a) and hydrophobic interactions by their alkyl group. Following adsorption, their –COOH group re-orient towards water, due to hydrophilicity of –COOH, enhancing polar, and Lewis acid-base interactions. The re-oriented –COOH has the potential to draw more feed water towards the membrane surface, thereby, decreasing WCA, and increasing γ_S^{tot}, leading to a low VFA S_{eff} and R_{Nut}. The mentioned first and second mechanisms are amplified by high VFA concentrations and the presence of higher carbon chain VFAs, e.g. C_5-C_8 than C_2-C_4 [35,73].

3.4. Surface free energy and Lewis acid-base component on membrane

The DPM exhibited γ_S^{tot} and Lewis-acid base (γ_S^{AB}) values of 14.1 and 0.10 mJ/m^2 concurrently (Fig. 5a). These were consistent with 15.5–15.8 mJ/m^2 for γ_S^{tot} and 0.12–0.14 for γ_S^{AB} in literature [49,60]. The γ_S^{tot} of the membranes NC_2-C_4, NC_5-C_8, and NC_2-C_8 (Fig. 5a) followed γ_S^{LW} trend discussed in Section 3.2 due to increasing γ_S^d, γ_S^p and γ_S^{AB} [67,74] (Fig. 3). The γ_S^{AB} of NC_2-C_4, NC_5-C_8, and NC_2-C_8 (Fig. 5a) increased, accounting for 0.7–8.5 % of γ_S^{tot}. The increased γ_S^{AB} values were mainly due to either protonated or dissociated VFAs. The γ_S^+ corresponded to 0.4–34 mJ/m^2 and contributed a greater portion of γ_S^{AB} compared to 0.02–1.8 mJ/m^2 of γ_S^- (Fig. 5b).

The increase in γ_S^+ is attributed to the acidity of protonated VFAs containing –COOH, whereas the γ_S^- is contributed by dissociated VFAs comprising $–COO^-$ [75,76]. Thus, the higher values of γ_S^+ than γ_S^- indicate that protonated VFAs permeated the membrane than dissociated VFAs, hence increasing VFA S_{eff}. Therefore, the increase in γ_S^d and γ_S^p discussed in Section 3.2 above was mainly due to more protonated VFAs permeating and interacting with the membrane. A previous study demonstrated that low feed pH levels (2–6) result in high protonated VFA flux whereas high pH levels (8–12) decrease VFA flux due to few quantities of protonated VFAs [35]. Thus, the feed pH plays an important role in VFA interaction with the membrane; however, investigating the effects of various feed pH is outside the scope of this research. Overall, the results indicate that VFAs increase γ_S^{tot} primarily through increasing γ_S^{LW} and γ_S^+ during VFA separation from nutrients via HMC.

The C_5-C_8 impacted the γ_S^+ 9.3-fold compared to C_2-C_4 (Fig. 5b). This effect is attributed to the C_5-C_8 higher hydrophobicity factor (expressed as octanol water partition coefficient, P_{ow}), which is 30 to 1600-fold that of C_2-C_4 [35]. As a result, C_5-C_8 extensively adsorbed on the membrane, leading to increased γ_S^+ due to their –COOH group compared to C_2_C_4 [67,75,76]. The higher γ_S^+ induced by C_5-C_8 indicates that, for equimolar VFAs, protonated C_5-C_8 generally interact and permeate the membrane more than C_2-C_4. The increased in γ_S^+on membrane surface γ_S^+ can attract Lewis bases e.g.·H_2O, SO_4^{2-}, $H_2PO_4^-$, NH_3 etc. from the feed to the membrane, resulting in decreased WCA, R_{Nut} and VFA S_{eff} [77]. However, for non-equimolar VFA concentrations, while the type of VFA affects γ_S^+, the specific concentration levels of C_2-C_4 or C_5-C_8 also play a substantial role.

3.5. Changing trend in membrane surface components due to feed composition

The B0, B1, and B2 feeds enhanced surface interactions. On average, γ_S^+ showed the most enhanced component, followed by γ_S^p, while γ_S^d and γ_S^- were the leas affected (Fig. 6).

The γ_S^+ increased to 1–3 orders of magnitude, whereas γ_S^d and γ_S^- changed by 1–2, and 0.1–7-fold, respectively. The increased γ_S^+ was discussed in Section 3.4 [42,67,78,79]. Despite the γ_S^+ changing by up to three orders of magnitude, γ_S^{tot} only increased maximally by 3-fold. Moreover, the enhancement factor of γ_S^{tot} followed a trend similar to γ_S^d, suggesting that γ_S^+ had less contribution to γ_S^{tot} than γ_S^d. Thus, the γ_S^+

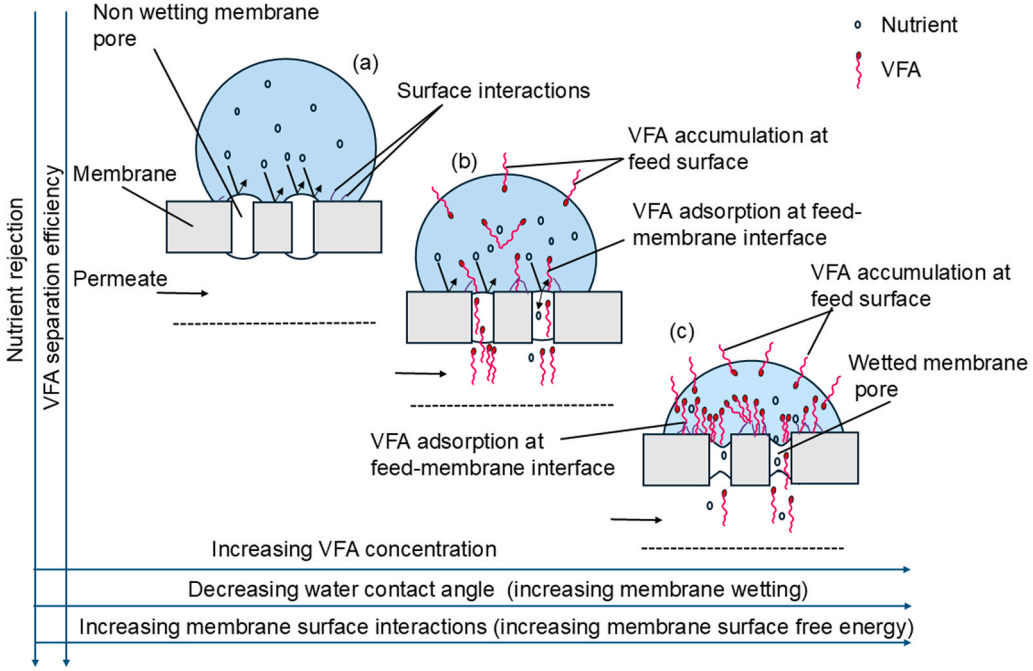

Fig. 4. Changes in WCA, γ_S^{tot}, VFA S_{eff} and nutrient rejection due to: (a) absence of VFA; (b) low VFA accumulation and adsorption on feed and membrane surfaces; and (c) high VFA accumulation and adsorption on feed and membrane surfaces.

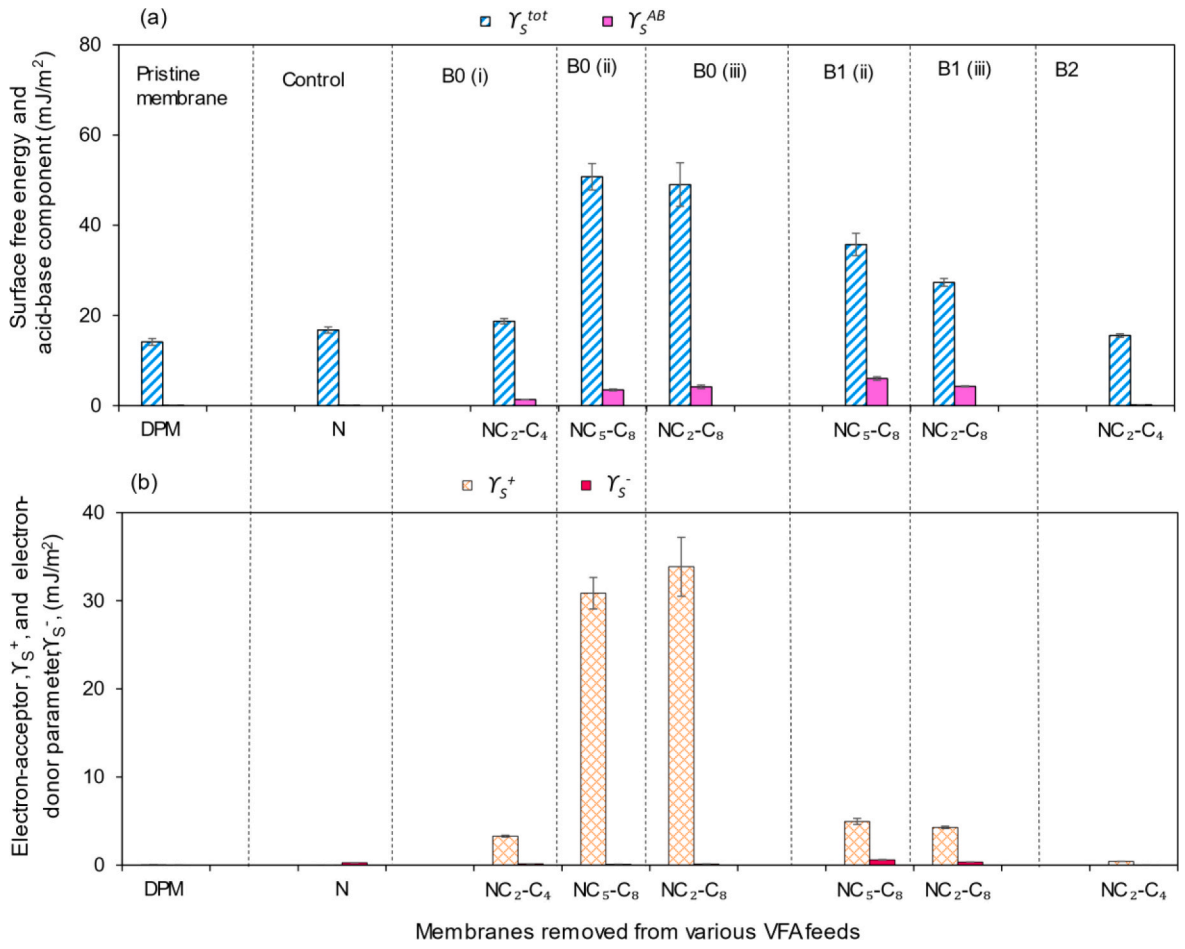

Fig. 5. (a) Surface free energy and Lewis acid-base component; (b) electron-pair acceptor (Lewis acid) and electron-pair donor (Lewis base) components.

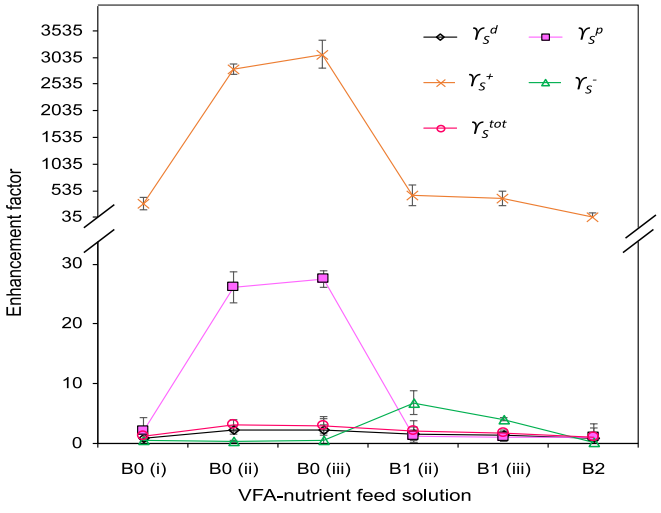

Fig. 6. Υ_S^d, Υ_S^p, Υ_S^+, and Υ_S^- enhancement factor of membranes exposed to VFA-nutrient feed solutions.

is an indication of protonated VFAs permeating the membrane but does not entirely account for interactions of other VFA atoms, such as alkyl carbon, which increases the Υ_S^{tot}. However, the extent of this alteration depends on the composition and concentration of VFAs in the feed.

3.6. Surface energies of membrane exposed to industrial FFW

The surface interactions of the membrane exposed to the FFW exhibited a trend similar to the membranes subjected to the synthetic feed solutions. Particularly, Υ_S^d and Υ_S^p accounted for 76 % and 24 % of the Υ_S^{LW} sequentially (Fig. 7). Overall, the Υ_S^d, Υ_S^p, and Υ_S^{AB} components contributed 63.9, 20.5, and 15.6 % of Υ_S^{tot}, respectively. The dominance of the Υ_S^d over Υ_S^p and Υ_S^{AB} suggests that during HMC, the dispersive interactions primarily alter the overall membrane surface properties. As a result, modifying Υ_S^d can substantially tune the membrane behavior for high VFA S_{eff} and R_{Nut}.

The membrane exhibited Υ_S^{AB}, Υ_S^+, and Υ_S^- values of 6.7, 10.0, and 1.1 mJ/m^2, respectively. The Υ_S^+, which was 12-fold the magnitude of Υ_S^-, contributed a greater portion of the Υ_S^{AB} due to protonated VFAs permeating the membrane (discussed in Section 3.4).

3.7. Nutrient rejection and VFA separation efficiency

The study explored the R_{Nut} and VFA S_{eff} alongside the changing Υ_S^{tot} of membranes exposed to various feeds.

3.8. Nutrient rejection

The nutrient rejection (R_{Nut}) declined from ~ 100 % to 94.5 % as Υ_S^{tot} increased from 16 to 51 mJ/m^2 (Fig. 8a). Increasing Υ_S^{tot} enhanced nutrient flux, leading to a decreased R_{Nut} (Fig. 8b). With the Control feed, R_{Nut} remained at 99.99 % (Fig. 8a). However, the presence of VFAs decreased R_{Nut}, depending on VFA concentration and composition. For example, C_2-C_4 (0.15 M total concentration) and C_5-C_8 (0.15 M total

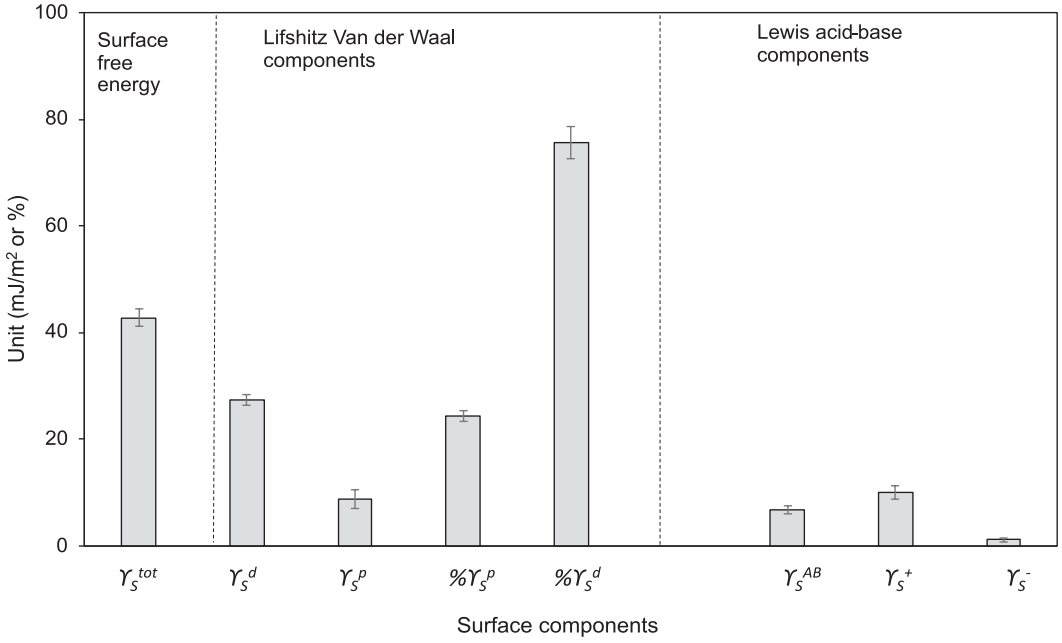

Fig. 7. Surface energies of membranes exposed to FFW during VFA separation via HMC.

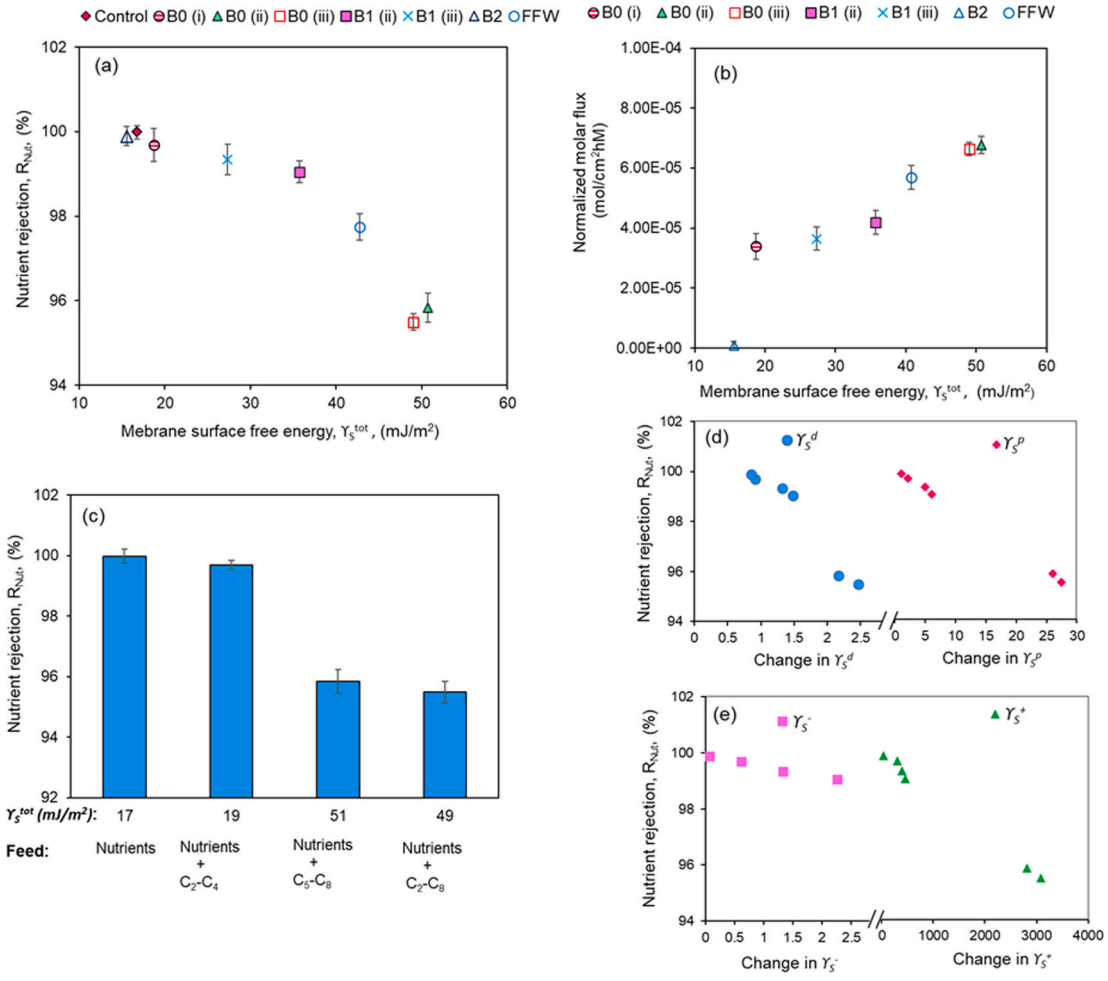

Fig. 8. Trend in Υ_S^{tot} and (a) R_{Nut}; (b) nutrient normalized molar flux; (c) VFA composition and R_{Nut}; (d) change in Υ_S^{d} and Υ_S^{p} relating to R_{Nut}; (e) change in Υ_S^{-} and Υ_S^{+} relating to R_{Nut}.

concentration) in B0 (i) and B0 (ii) (Table 1) respectively decreased R_{Nut} to 99.7 % and 95.8 %, compared to 99.9 % and 99.1 % obtained from B2 (0.08 M total concentration of C_2-C_4) and B1 (ii) (0.019 M total concentration of C_5-C_8) (Fig. 8a, and c). The C_5-C_8, due to increased γ_S^{LW} and γ_S^+ relative to C_2-C_4, intensified the nutrient flux, resulting in a decreased R_{Nut}. This undesirable situation, caused by the VFAs themselves, though not yet reported in the literature, can deteriorate VFA selectivity over nutrients in HMC systems, especially, for separating high-concentration C_5-C_8. For instance, about 0.02–0.04 M of C_6 and C_8 similar to feed B0 (ii) have been produced from FFW [19]. In such high concentrations, the stability of the γ_S^{tot} and WCA above 90° are important for high VFA S_{eff} and R_{Nut}.

The decline in R_{Nut} is associated with decreased WCA (Fig. 2), and increased γ_S^{tot} (Fig. 5a). Thus, the VFAs caused partial membrane wetting, leading to a decreased R_{Nut}. However, the decreasing R_{Nut} was gradual (~100 % to 99.1 %) from 16 mJ/m^2 (WCA 125°) to 36 mJ/m^2 (WCA 102°), but a sharp drop occurred at 43 mJ/m^2. This transition indicates that changes in γ_S^{tot} do not equivalently affect R_{Nut} during HMC operation. In this research, $\gamma_S^{tot} \leq 36$ mJ/m^2 and WCA $\geq 102°$ are considered crucial for achieving R_{Nut} above 99 %. This crucial region attained a highly stable nutrient rejection. Previous studies showed that ion rejection decreased from >99.9 % to 95 % as WCA declined from over 140° to below 100° [43,44,64–66]. Since the γ_S^d and γ_S^p (γ_S^{LW}) contributed to >80 % and aligned closely with γ_S^{tot} than γ_S^+, and γ_S^- (γ_S^{AB}) (Fig. 6), the impact of γ_S^{tot} on R_{Nut} is predominantly due to changes in γ_S^{LW} than γ_S^{AB}.

Individually, γ_S^d, γ_S^p, γ_S^+, and γ_S^- increased as R_{Nut} decreased (Fig. 8d–e). This indicates that the interaction of VFAs with the membrane surface undesirably enhanced nutrient flux through the membrane. This effect is attributed to the combined increase in γ_S^{tot} and the decrease in WCA, as discussed earlier. However, at the same R_{Nut}, the components γ_S^p and γ_S^+ changed sharply than γ_S^d and γ_S^-. The pronounced increase in γ_S^+ and γ_S^p suggests that the Lewis acid and polar components of the hydrophobic membrane are more sensitive to the presence of VFAs on the membrane surface due to the –COOH group of the VFAs. Nonetheless, similar to γ_S^{tot} in Fig. 8a, the changes in γ_S^d, γ_S^p, γ_S^+, and γ_S^- were not proportional to changes in R_{Nut}. For instance, as R_{Nut} decreased slightly from 99.9 % to 99.1 %, γ_S^d, γ_S^p, γ_S^+, and γ_S^- enhanced from ~1 to 1.5, 1.1 to 6.1, 39 to 453, and 0.1 to 2.3-fold respectively (Fig. 8d–e) respectively.

Though Ca^{2+}, Mg^{2+}, Cl^-, and Na^+ were excluded from synthetic solutions, their rejections in FFW were similar to K^+, NH_4^+, NO_3^-, and $H_2PO_4^-$ (Fig. S1). The results imply that under the same conditions of this study, the magnitude of the nutrient rejection measured from the synthetic solutions would not be substantially different if the other inorganic ions (i.e Ca^{2+}, Mg^{2+}, Cl^-, and Na^+) were added. These results align with previous study where PTFE membrane blocked most of the nutrients and inorganic ions in the feed during HMC applied for VFA separation [29].

3.9. VFA separation efficiency

The membranes achieved VFA S_{eff} ranging from 40 % to 73 % (Fig. 9). For the same type of VFAs, a similar γ_S^{tot} resulted in comparable S_{eff} values. For instance, the S_{eff} of C_2-C_4 in B2 and B0 (i) were comparable due to the similar γ_S^{tot} values (16 and 19 mJ/m^2) of their corresponding membranes. For the same concentration as in B 0 (i) and B0 (ii) at pH 5, C_5-C_8 attained higher S_{eff} than C_2-C_4. As indicated by the high γ_S^d, γ_S^p, γ_S^+, and γ_S^{tot} induced by C_5-C_8, a superior interaction between the protonated C_5-C_8 and the PTFE membrane resulted in higher flux, leading to enhanced S_{eff} than C_2-C_4.

Although a higher γ_S^{tot} indicates increased membrane-VFA interaction, and high VFA S_{eff}, a continuous increase in γ_S^{tot} combined with WCA < 90°, inhibited the S_{eff}. This was more prominent in feeds B1 (ii) and B0 (ii) containing C_5-C_8 . The S_{eff} of C_5-C_8 decreased by 8 % when the γ_S^{tot} increased by 41 % from 36 mJ/m^2 (Fig. 9) together with decreased WCA from 102° to 46° (Fig. 2). Additionally, the S_{eff} of C_2-C_8 in B1 (iii) and B0 (iii) declined by 19 % as the γ_S^{tot} increased by 82 % from 27 mJ/m^2 whilst the WCA declined from 106° to 44°. The HMC requires stable membrane hydrophobicity, ensuring that vapors of protonated VFAs permeate the membrane while nutrients remain in the feed. This increases the VFA S_{eff} and R_{Nut} [29,37,39]. However, as γ_S^{tot} continuously increased and WCA decreased, especially below 90°, fewer protonated VFA vapors were transported (Fig. 4b, and c), leading to a lower VFA S_{eff}. (Fig. 9).

A previous study on HMC prevented nutrient and VFA losses while separating 18–25 % of C_2-C_5 [29]. Nevertheless, this current research indicates that a decline in WCA (Fig. 2) and an increase in γ_S^{tot} (Fig. 5) are more pronounced in feed containing high concentration C_5-C_8 compared to C_2-C_4. Therefore, although HMCs are widely applied to separate VFAs from nutrients in FFW, and anaerobically digested media, C_5-C_8 can adversely affect overall VFA S_{eff} and R_{Nut}. In this study, the desirable conditions for selectively separating VFAs ($S_{eff} \geq 99$ %) while minimizing nutrient contamination in the permeate were found to be a γ_S^{tot} of ≤36 mJ/m^2 and a WCA of ≥102°. However, changes in γ_S^d compared to γ_S^p, γ_S^+, or γ_S^- closely follow γ_S^{tot} as discussed in Section 3.5 (Fig. 6). Therefore, the effect of γ_S^{tot} on R_{Nut} and VFA S_{eff} demonstrated in Figs. 8a and 9 is mainly influenced by γ_S^d than the other surface

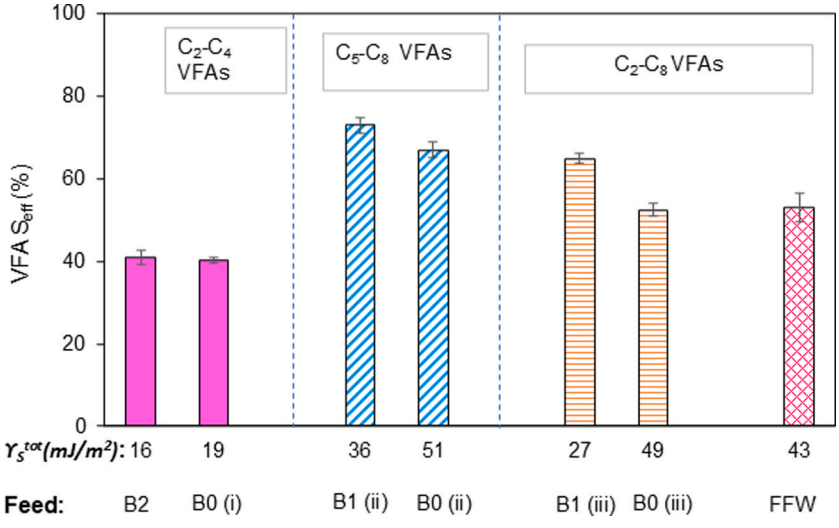

Fig. 9. Υ_S^{tot} and VFA S_{eff}.

components examined in this study.

3.10. Implications and large-scale applications

The results of this study indicate that VFA interactions with hydrophobic membrane utilized in HMC influence WCA and Υ_S^{tot}, which in turn can negatively affect VFA S_{eff}, and R_{Nut}. Thus, an increase in VFA concentration, especially C_5-C_8, leads to stronger VFA adsorption on the membrane surface, disrupting optimal WCA, Υ_S^{tot}, VFA S_{eff}, and R_{Nut}.

One strategy to optimize WCA, and Υ_S^{tot} is by controlling the concentration of protonated VFAs in the feed. Due to high hydrophobicity (expressed as octanol–water partition coefficient) of protonated VFAs [35], they readily and strongly interact with hydrophobic membranes than dissociated VFAs. Therefore, based on VFA pKa (4.75–4.89) and Eq. (9), controlling the feed pH to decrease the percentage of protonated VFAs [16,37,80], can mitigate the detrimental effects of high concentration VFAs on WCA and Υ_S^{tot}. For example, Eq. (9) indicates that adjusting B0 (ii) feed pH from 5 to 6 decreases protonated C_5-C_8 in the feed from 40 % to ~7 %, respectively. Decreasing protonated VFA concentration minimizes their disruptive impact on feed (water) surface tension or the cohesive forces between water molecules (discussed in Section 3.3) [68–70], and reduces excessive VFA adsorption (Fig. 2b), thereby, decreasing the adverse effects on WCA and Υ_S^{tot}, VFA S_{eff} (both C_5-C_8 and C_2-C_4), and R_{Nut}. It is important to note that though increasing feed pH does not compromise VFA S_{eff} (amount of protonated VFA separated per initial amount in the feed) [16,81], WCA, Υ_S^{tot}, and and R_{Nut}, it decreases VFA flux due to less amount of protonated VFAs in the feed. Therefore, after separating a substantial amount of protonated VFAs from the feed via HMC, the feed pH can be re-adjusted (decreased) to convert some amount of dissociated VFAs into tolerable concentration of protonated VFAs, allowing further separation without disrupting optimal WCA, and Υ_S^{tot}.

Another strategy to enhance WCA is direct feed dilution. High feed surface tension improves WCA [82,83]. This issue is particularly relevant for VFAs with high surfactant activity, such as C_5-C_8. Therefore, diluting the feed solution to decrease VFA concentrations can minimize negative impact of VFAs on feed (water) cohesive forces and surface tension [68–70]. In this study, feed B1 (ii) with dilute concentrations of C_5-C_8 had minimal disruptive effect on WCA (Fig. 2a), Υ_S^{tot} (Fig. 5a), VFA S_{eff} (Fig. 9), and R_{Nut} (Fig. 8a) compared to B0 (ii) with high concentrations. However, this dilution approach may not be compatible with systems coupling HMC with anaerobic digestion reactor. Thus, it may be more practical for standalone HMC treating FFW post-fermentation or post-digestion.

Membrane modifications which adjust membrane surface roughness, and chemistry offer another route for increasing WCA and decreasing Υ_S^{tot} as strategy for optimization [82,83]. For instance, membranes surface treated with fluorosilanes, Hyflon® AD, or hydrophobic nanoparticles tripled surface roughness, increased WCA from 125° to ~163°, maintained >99 % salt rejection, and decreased Υ_S^{tot} from ~17 to 6 mJ/m^2 in some cases [84–86]. However, achieving superhydrophobicity can also lead to excessive VFA adsorption, again disrupting WCA and Υ_S^{tot}. Hence, maintaining a balance between WCA and Υ_S^{tot} is crucial.

As awareness on circular economy grows, recovering high-purity VFAs can enhance their commercial and industrial applications while minimizing environmental pollution of FW [2,8,9,87–89]. Considering the 1.3 billion tonnes of annual FW generation [90], and up to 80 % (w/w VFA/Volatile solid yield), about 0.22 billion tonnes of VFAs can be globally produced and separated from FFW [91,92] for large-scale industrial applications [8,93]. In this case, increasing the membrane area to improve the 40–73 % VFA S_{eff} obtained in this study can promote large-scale separation [16,29]. Additionally, this study demonstrates that optimal WCA and Υ_S^{tot} are important for separating VFAs from FFW with less nutrient contamination. Thus, these findings highlight the pivotal role of WCA and Υ_S^{tot} in enhancing separation between VFAs and nutrients from FFW via HMC while aligning with circular economy, environmental sustainability and minimizing adverse environmental impacts of food waste.

4. Conclusions

PTFE HMC was applied to separate VFAs from nutrients in synthetic solutions and industrial FFW. The membrane surface interactions were also analyzed. Across all feed solutions, the HMC separated 40–73 % VFAs to the permeate with 0.01–5.5 % nutrient contamination, and rejected at least 95 % of nutrients in the feed. Water contact angle (WCA), and membrane surface free energy (Υ_S^{tot}) have pivotal impacts on VFA separation efficiency (S_{eff}) and nutrient rejection (R_{Nut}). In this study, the optimal conditions for separating VFAs from FFW into the HMC permeate while minimizing nutrient contamination and achieving $R_{Nut} \geq 99$ % were found to be $\Upsilon_S^{tot} \leq 36$ mJ/m^2 and WCA $\geq 102°$. The intensity of Υ_S^{tot} was primarily contributed by Υ_S^d. The VFAs dominantly increased Υ_S^d and Υ_S^p compared to nutrients, implying the membrane's superior selectivity for VFAs over nutrients, hence higher VFA separation to the permeate. The Υ_S^+ was the most sensitive to VFA feed solutions, whereas Υ_S^d was the least susceptible. A higher Υ_S^+ compared to Υ_S^- indicates predominant permeation of protonated VFAs through the membrane than dissociated VFAs. Additionally, C_5-C_8 induced a higher Υ_S^+ compared to C_2-C_4, indicating that, more protonated C_5-C_8 permeated the membrane than C_2-C_4. Overall, the study highlights that VFA interactions with hydrophobic membrane used in HMC influence WCA, and Υ_S^{tot} which can adversely affect separation between VFAs and nutrients. Additionally, VFA composition and concentration in HMC feed impact the magnitude of WCA, and Υ_S^{tot}, influencing R_{Nut} and VFA S_{eff}. Increasing C_5-C_8 concentration disrupts WCA, and Υ_S^{tot}, VFA S_{eff}, and R_{Nut} than C_2-C_4 at the same concentration. Therefore, in HMCs applied for VFA separation from FFW, optimizing Υ_S^{tot} and WCA for specific VFA feed concentration and composition are crucial for achieving optimal R_{Nut} and VFA S_{eff}. Additionally, FFW could contain other organics such as proteins, and polysaccharides which can also interact with the membrane, depending on their concentration. Therefore, future studies should comprehensively investigate membrane interactions with other organics to help minimize potential membrane fouling.

CRediT authorship contribution statement

Francis Kotoka: Writing – review & editing, Writing – original draft, Visualization, Validation, Methodology, Investigation, Formal analysis, Data curation, Conceptualization. **Leonardo Gutierrez:** Writing – review & editing, Supervision, Software, Resources, Project administration, Funding acquisition, Conceptualization. **Emile Cornelissen:** Writing – review & editing, Supervision, Software, Resources, Project administration, Funding acquisition, Conceptualization.

Funding

This study was funded by the European Union's Horizon 2020 research and innovation program under grant agreement no 101000527 through the RUSTICA research project.

Declaration of competing interest

The authors declare that they have no known competing financial interests or personal relationships that could have appeared to influence the work reported in this paper.

Acknowledgements

Francis Kotoka acknowledges John Buffel and Saskia Van der Looven for their administrative supports. He also acknowledges the grant provided by the European Union's Horizon 2020 through the RUSTICA Project.

Appendix A. Supplementary data

Supplementary data to this article can be found online at https://doi.org/10.1016/j.seppur.2025.133840.

Data availability

Data will be made available on request.

References

[1] UN report: one-third of world's food wasted annually, at great economic, environmental cost | | UN News. https://news.un.org/en/story/2013/09/448652. Accessed 19 Jun 2022.

[2] R. Kalnina, I. Demjanenko, D. Gorbacenko, Nutrient analysis of food waste from ships' greywater in the Baltic Sea, Water 13 (2021) 2421, https://doi.org/10.3390/W13172421.

[3] G.K. Hassan, J. Massanet-Nicolau, R. Dinsdale, et al., A novel method for increasing biohydrogen production from food waste using electrodialysis, Int. J. Hydrogen Energy 44 (2019) 14715–14720, https://doi.org/10.1016/j.ijhydene.2019.04.176.

[4] C. Bak, Y.M. Yun, J.H. Kim, S. Kang, Electrodialytic separation of volatile fatty acids from hydrogen fermented food wastes, Int. J. Hydrogen Energy 44 (2019) 3356–3362, https://doi.org/10.1016/j.ijhydene.2018.07.134.

[5] Jon Jones 2021_Continuous recovery and enhanced yields of volatile fatty acids from acontinually-fed 100 L food waste bioreactor by filtration andelectrodialysis.pdf.

[6] M.P. Zacharof, R.W. Lovitt, Recovery of volatile fatty acids (VFA) from complex waste effluents using membranes, Water Sci. Technol. 69 (2014) 495–503, https://doi.org/10.2166/wst.2013.717.

[7] M.P. Zacharof, R.W. Lovitt, Complex effluent streams as a potential source of volatile fatty acids, Waste Biomass Valoriz. 4 (2013) 557–581, https://doi.org/10.1007/s12649-013-9202-6.

[8] S. Aghapour Aktij, A. Zirehpour, A. Mollahosseini, et al., Feasibility of membrane processes for the recovery and purification of bio-based volatile fatty acids: A comprehensive review, J. Ind. Eng. Chem. 81 (2020) 24–40, https://doi.org/10.1016/j.jiec.2019.09.009.

[9] B. Eryildiz, T.MJ. Lukitawesa, Effect of pH, substrate loading, oxygen, and methanogens inhibitors on volatile fatty acid (VFA) production from citrus waste by anaerobic digestion, Bioresour. Technol. 302 (2020) 122800, https://doi.org/10.1016/J.BIORTECH.2020.122800.

[10] C. Huang, T. Xu, Y. Zhang, et al., Application of electrodialysis to the production of organic acids: State-of-the-art and recent developments, J. Memb. Sci. 288 (2007) 1–12.

[11] H. Takahashi, K. Ohba, K.I. Kikuchi, Sorption of mono-carboxylic acids by an anion-exchange membrane, Biochem. Eng. J. 16 (2003) 311–315, https://doi.org/10.1016/S1369-703X(03)00077-9.

[12] H. Takahashi, K. Ohba, K.-I. Kikuchi, Sorption of di- and tricarboxylic acids by an anion-exchange membrane, J. Memb. Sci. 222 (2003) 103–111, https://doi.org/10.1016/S0376-7388(03)00259-X.

[13] P. Boyaval, C. Corre, Production of propionic acid, 1995.

[14] J. McMurry, Organic Chemistry, 5th ed., Brooks Cole, Pacific Grove, California, 2000.

[15] World Bank (2016) Trends in Solid Waste Management. https://datatopics.worldbank.org/what-a-waste/trends_in_solid_waste_management.html. Accessed 19 Dec 2023.

[16] F. Kotoka, L. Gutierrez, A. Verliefde, E. Cornelissen, Selective separation of nutrients and volatile fatty acids from food wastes using electrodialysis and membrane contactor for resource valorization, J. Environ. Manage. 354 (2024) 120290, https://doi.org/10.1016/J.JENVMAN.2024.120290.

[17] R.J. Jones, R. Fernández-Feito, J. Massanet-Nicolau, et al., Continuous recovery and enhanced yields of volatile fatty acids from a continually-fed 100 L food waste bioreactor by filtration and electrodialysis, Waste Manag. 122 (2021) 81–88, https://doi.org/10.1016/j.wasman.2020.12.032.

[18] J.M.B. Domingos, G.A. Martinez, A. Scoma, et al., Effect of operational parameters in the continuous anaerobic fermentation of cheese whey on titers, yields, productivities, and microbial community structures, ACS Sustain. Chem. Eng. 5 (2017) 1400–1407, https://doi.org/10.1021/ACSSUSCHEMENG.6B01901/SUPPL_FILE/SC6B01901_SI_002.XLSX.

[19] J.M.B. Domingos, S. Puccio, G.A. Martinez, et al., Cheese whey integrated valorisation: Production, concentration and exploitation of carboxylic acids for the production of polyhydroxyalkanoates by a fed-batch culture, Chem. Eng. J. 336 (2018) 47–53, https://doi.org/10.1016/J.CEJ.2017.11.024.

[20] D. Pleissner, F. Demichelis, S. Mariano, et al., Direct production of lactic acid based on simultaneous saccharification and fermentation of mixed restaurant food waste, J. Clean. Prod. 143 (2017) 615–623, https://doi.org/10.1016/j.jclepro.2016.12.065.

[21] M. Faucher, É. Serre, M.-È. Langevin, et al., Drastic energy consumption reduction and ecoefficiency improvement of cranberry juice deacidification by electrodialysis with bipolar membranes at semi-industrial scale: Reuse of the recovery solution, J. Memb. Sci. 555 (2018) 105–114, https://doi.org/10.1016/j.memsci.2018.02.041.

[22] A. Scoma, F. Varela-Corredor, L. Bertin, et al., Recovery of VFAs from anaerobic digestion of dephenolized olive mill wastewaters by electrodialysis, Sep. Purif. Technol. 159 (2016) 81–91, https://doi.org/10.1016/j.seppur.2015.12.029.

[23] X. Zhu, A. Leininger, D. Jassby, et al., Will membranes break barriers on volatile fatty acid recovery from, Anaerobic Digestion 1 (2021) 141–153, https://doi.org/10.1021/acsestengg.0c00081.

[24] B. Sniatala, T.A. Kurniawan, D. Sobotka, et al., Macro-nutrients recovery from liquid waste as a sustainable resource for production of recovered mineral fertilizer: Uncovering alternative options to sustain global food security cost-effectively, Sci. Total Environ. 856 (2023) 159283, https://doi.org/10.1016/J.SCITOTENV.2022.159283.

[25] A. Sarrion, E. Diaz, M.A. de la Rubia, A.F. Mohedano, Fate of nutrients during hydrothermal treatment of food waste, Bioresour. Technol. 342 (2021) 125954, https://doi.org/10.1016/J.BIORTECH.2021.125954.

[26] I. Idowu, L. Li, J.R.V. Flora, et al., Hydrothermal carbonization of food waste for nutrient recovery and reuse, Waste Manag. 69 (2017) 480–491, https://doi.org/10.1016/J.WASMAN.2017.08.051.

[27] V.D. Talnikar, Y.S. Mahajan, Recovery of acids from dilute streams : A review of process technologies, Korean J. Chem. Eng. 31 (2014) 1720–1731, https://doi.org/10.1007/s11814-014-0202-4.

[28] C.M. Mehta, W.O. Khunjar, V. Nguyen, et al., Technologies to recover nutrients from waste streams: A critical review, Crit. Rev. Environ. Sci. Technol. 45 (2015) 385–427.

[29] R. Chalmers Brown, R. Tuffou, J. Massanet Nicolau, et al., Overcoming nutrient loss during volatile fatty acid recovery from fermentation media by addition of electrodialysis to a polytetrafluoroethylene membrane stack, Bioresour. Technol. 301 (2020) 122543, https://doi.org/10.1016/j.biortech.2019.122543.

[30] E. Reyhanitash, S.R.A. Kersten, Schuur B, Recovery of Volatile Fatty Acids from Fermented Wastewater by Adsorption, 2017. https://doi.org/10.1021/acssuschemeng.7b02095.

[31] A. Talebi, Y.S. Razali, N. Ismail, et al., Selective adsorption and recovery of volatile fatty acids from fermented landfill leachate by activated carbon process, Sci. Total Environ. 707 (2020) 134533, https://doi.org/10.1016/J.SCITOTENV.2019.134533.

[32] F. Rizzioli, F. Battista, D. Bolzonella, N. Frison, Volatile fatty acid recovery from anaerobic fermentate: Focusing on adsorption and desorption performances, Ind. Eng. Chem. Res. 60 (2021) 13701–13709, https://doi.org/10.1021/ACS.IECR.1C03280/ASSET/IMAGES/LARGE/IE1C03280_0004.JPEG.

[33] N. Lammari, M. Tarhini, K. Miladi, et al., Encapsulation methods of active molecules for drug delivery, Drug Deliv. Dev. Therap. Syst. 289–306 (2020), https://doi.org/10.1016/B978-0-12-819838-4.00008-0.

[34] A. Gugliuzza, A. Basile, Membrane contactors: Fundamentals, membrane materials and key operations, Handbook Memb. React. 2 (2013) 54–106, https://doi.org/10.1533/9780857097347.1.54.

[35] H. Lee, S.-J. Im, C. Kim, Jang a,, Relative selectivity of short- and medium-chain fatty acids in hydrophobic membrane for resource recovery in wastewater: Effects of supported liquid, feed pH, and membrane pores, Chem. Eng. J. 446 (2022) 137258, https://doi.org/10.1016/J.CEJ.2022.137258.

[36] K. Sofiya, E. Poonguzhali, A. Kapoor, et al., Separation of carboxylic acids from aqueous solutions using hollow fiber membrane contactors, J. Memb. Sci. Res. 5 (2019) 233–239. https://doi.org/10.22079/JMSR.2018.88804.1199.

[37] A.E. Tugtas, Recovery of volatile fatty acids via membrane contactor using flat membranes: Experimental and theoretical analysis, Waste Manag. 34 (2014) 1171–1178, https://doi.org/10.1016/J.WASMAN.2014.01.020.

[38] S. Aydin, H. Yesil, A.E. Tugtas, Recovery of mixed volatile fatty acids from anaerobically fermented organic wastes by vapor permeation membrane contactors, Bioresour. Technol. 250 (2018) 548–555, https://doi.org/10.1016/J.BIORTECH.2017.11.061.

[39] H. Ravishankar, P. Dessì, S. Trudu, et al., Silicone membrane contactor for selective volatile fatty acid and alcohol separation, Process Saf. Environ. Prot. 148 (2021) 125–136, https://doi.org/10.1016/J.PSEP.2020.09.052.

[40] Y. Zhang, S. Paepen, L. Pinoy, et al., Selectrodialysis: Fractionation of divalent ions from monovalent ions in a novel electrodialysis stack, Sep. Purif. Technol. 88 (2012) 191–201, https://doi.org/10.1016/j.seppur.2011.12.017.

[41] J.M. Schuster, C.E. Schvezov, M.R. Rosenberger, Analysis of the results of surface free energy measurement of Ti6Al4V by different methods, Procedia Mater. Sci. 8 (2015) 732–741, https://doi.org/10.1016/J.MSPRO.2015.04.130.

[42] B.S. Jańczuk, T. Bialopiotrowicz, A. Zdziennicka, Some remarks on the components of the liquid surface free energy, J. Colloid Interface Sci. 211 (1999) 96–103, https://doi.org/10.1006/JCIS.1998.5990.

[43] L.F. Dumée, S. Gray, M. Duke, et al., The role of membrane surface energy on direct contact membrane distillation performance, Desalination 323 (2013) 22–30, https://doi.org/10.1016/J.DESAL.2012.07.012.

[44] L. Dumée, J.L. Campbell, K. Sears, et al., The impact of hydrophobic coating on the performance of carbon nanotube bucky-paper membranes in membrane distillation, Desalination 283 (2011) 64–67, https://doi.org/10.1016/J.DESAL.2011.02.046.

[45] P. Nuchnoi, T. Yano, N. Nishio, S. Nagai, Extraction of volatile fatty acids from diluted aqueous solution using a supported liquid membrane, J. Ferment. Technol. 65 (1987) 301–310, https://doi.org/10.1016/0385-6380(87)90092-6.

[46] R.J. Jones, J. Massanet-Nicolau, R. Fernandez-Feito, et al., Fermentative volatile fatty acid production and recovery from grass using a novel combination of solids separation, pervaporation, and electrodialysis technologies, Bioresour. Technol. 342 (2021) 125926, https://doi.org/10.1016/J.BIORTECH.2021.125926.

[47] A. Royaux, A. El Haitami, O. Fichet, S. Cantin, Surface free-energy determination of copper wire using a large range of model liquids, SN Appl. Sci. 2 (2020) 1–9, https://doi.org/10.1007/S42452-019-1828-Y/FIGURES/7.
[48] D.K. Owens, R.C. Wendt, Estimation of the surface free energy of polymers, J. Appl. Polym. Sci. 13 (1969) 1741–1747, https://doi.org/10.1002/APP.1969.070130815.
[49] S. Lee, J.S. Park, T.R. Lee, The wettability of fluoropolymer surfaces: Influence of surface dipoles, Langmuir 24 (2008) 4817–4826, https://doi.org/10.1021/LA700902H/ASSET/IMAGES/MEDIUM/LA700902HN00001.GIF.
[50] M. Yao, L.D. Tijing, G. Naidu, et al., A review of membrane wettability for the treatment of saline water deploying membrane distillation, Desalination 479 (2020) 114312, https://doi.org/10.1016/J.DESAL.2020.114312.
[51] J. Comyn, F. De Buyl, C. Subramanian, The effect of contact with PTFE tape on the moisture cure of an alkoxysilicone sealant, Int. J. Adhes. Adhes. 22 (2002) 331–336, https://doi.org/10.1016/S0143-7496(02)00012-X.
[52] P. Wei, A. Xia, Q. Liao, et al., Enhancing fermentative hydrogen production with the removal of volatile fatty acids by electrodialysis, Bioresour. Technol. 263 (2018) 437–443, https://doi.org/10.1016/j.biortech.2018.05.030.
[53] Y. Zhang, J. Bai, J. Zuo, Performance and mechanisms of medium-chain fatty acid production by anaerobic fermentation of food waste without external electron donors, Bioresour. Technol. 374 (2023) 128735, https://doi.org/10.1016/J.BIORTECH.2023.128735.
[54] E. Kaya, A. Hasanoğlu, Removal of acetic acid from aqueous post-fermentation streams and fermented beverages using membrane contactors, J. Chem. Technol. Biotechnol. (2022), https://doi.org/10.1002/JCTB.7100.
[55] M. Parchami, C. Uwineza, O.H. Ibeabuchi, et al., Membrane bioreactor assisted volatile fatty acids production from agro-industrial residues for ruminant feed application, Waste Manag. 170 (2023) 62–74, https://doi.org/10.1016/J.WASMAN.2023.07.032.
[56] L. Wu, W. Wei, Z. Chen, et al., Medium chain fatty acids production from anaerobic fermentation of food wastes: The role of fermentation pH in metabolic pathways, Chem. Eng. J. 472 (2023) 144824, https://doi.org/10.1016/J.CEJ.2023.144824.
[57] X. Vecino, M. Reig, O. Gibert, et al., Integration of monopolar and bipolar electrodialysis processes for tartaric acid recovery from residues of the winery industry, ACS Sustain. Chem. Eng. 8 (2020) 13387–13399, https://doi.org/10.1021/ACSSUSCHEMENG.0C04166/ASSET/IMAGES/MEDIUM/SC0C04166_0009.GIF.
[58] A.T. Ren, L.K. Abbott, Y. Chen, et al., Nutrient recovery from anaerobic digestion of food waste: impacts of digestate on plant growth and rhizosphere bacterial community composition and potential function in ryegrass, Biol. Fertil. Soils 56 (2020) 973–989, https://doi.org/10.1007/S00374-020-01477-6/TABLES/3.
[59] D. Janssen, R. De Palma, S. Verlaak, et al., Static solvent contact angle measurements, surface free energy and wettability determination of various self-assembled monolayers on silicon dioxide, Thin Solid Films 515 (2006) 1433–1438, https://doi.org/10.1016/J.TSF.2006.04.006.
[60] A. Zdziennicka, J. Krawczyk, K. Szymczyk, B. Jańczuk, Components and parameters of liquids and some polymers surface tension at different temperature, Colloids Surf. A Physicochem. Eng. Asp. 529 (2017) 864–875, https://doi.org/10.1016/J.COLSURFA.2017.07.002.
[61] F.M. Fowkes, M.B. Kaczinski, D.W. Dwight, Characterization of polymer surface sites with contact angles of test solutions. 1. Phenol and iodine adsorption from CH2I2 onto PMMA films, Langmuir 7 (1991) 2464–2470, https://doi.org/10.1021/LA00059A012/ASSET/LA00059A012.FP.PNG_V03.
[62] L. Zhang, S.S. Hu, L. Zhang, et al., Wettability alteration by novel betaines at polymer–aqueous solution interfaces, Appl. Surf. Sci. 355 (2015) 868–877, https://doi.org/10.1016/J.APSUSC.2015.07.188.
[63] F.A. Ogunmokun, R. Wallach, Effect of surfactant surface and interfacial tension reduction on infiltration into hydrophobic porous media, Geoderma 441 (2024) 116735, https://doi.org/10.1016/J.GEODERMA.2023.116735.
[64] L. Dumée, V. Germain, K. Sears, et al., Enhanced durability and hydrophobicity of carbon nanotube bucky paper membranes in membrane distillation, J. Memb. Sci. 376 (2011) 241–246, https://doi.org/10.1016/J.MEMSCI.2011.04.024.
[65] L. Dumée, K. Sears, J. Schütz, et al., Carbon nanotube based composite membranes for water desalination by membrane distillation, Desalination Water Treat. 17 (2010) 72–79, https://doi.org/10.5004/DWT.2010.1701.
[66] L.F. Dumée, K. Sears, J. Schütz, et al., Characterization and evaluation of carbon nanotube Bucky-paper membranes for direct contact membrane distillation, J. Memb. Sci. 351 (2010) 36–43, https://doi.org/10.1016/J.MEMSCI.2010.01.025.
[67] C.J. van Oss (2006) Interfacial forces in aqueous media, second edition. Interfacial Forces in Aqueous Media, Second Edition 1–438. https://doi.org/10.1201/9781420015768/INTERFACIAL-FORCES-AQUEOUS-MEDIA-CAREL-VAN-OSS.
[68] T. Xu, V. Rodriguez-Martinez, S.N. Sahasrabudhe, et al., Effects of temperature, time and composition on food oil surface tension, Food Biophys. 12 (2017) 88–96, https://doi.org/10.1007/S11483-016-9466-Z/METRICS.
[69] E. Álvarez, G. Vázquez, M. Sánchez-Vilas, et al., Surface tension of organic acids + water binary mixtures from 20 °C to 50 °C, J. Chem. Eng. Data 42 (1997) 957–960, https://doi.org/10.1021/JE970025M.
[70] F. Suárez, C.M. Romero, Apparent molar volume and surface tension of dilute aqueous solutions of carboxylic acids, J. Chem. Eng. Data 56 (2011) 1778–1786, https://doi.org/10.1021/JE1002829.
[71] S. Badban, A.E. Hyde, C.M. Phan, Hydrophilicity of nonanoic acid and its conjugate base at the air/water interface, ACS Omega 2 (2017) 5565–5573, https://doi.org/10.1021/ACSOMEGA.7B00960/ASSET/IMAGES/LARGE/AO-2017-00960G_0008.JPEG.
[72] Z. He, F. Ning, F. Mi, et al., Molecular dynamics study on the spontaneous adsorption of aromatic carboxylic acids to methane hydrate surfaces: Implications for hydrate antiagglomeration, Energy Fuel 36 (2022) 3628–3639, https://doi.org/10.1021/ACS.ENERGYFUELS.2C00347/ASSET/IMAGES/LARGE/EF2C00347_0012.JPEG.
[73] B.A. Wellen, E.A. Lach, H.C. Allen, Surface pKa of octanoic, nonanoic, and decanoic fatty acids at the air–water interface: Applications to atmospheric aerosol chemistry, PCCP 19 (2017) 26551–26558, https://doi.org/10.1039/C7CP04527A.
[74] A. Rudawska, I. Danczak, M. Müller, P. Valasek, The effect of sandblasting on surface properties for adhesion, Int. J. Adhes. Adhes. 70 (2016) 176–190, https://doi.org/10.1016/J.IJADHADH.2016.06.010.
[75] S.R. Holmes-Farley, R.H. Reamey, T.J. McCarthy, et al., Acid-base behavior of carboxylic acid groups covalently attached at the surface of polyethylene: The usefulness of contact angle in following the ionization of surface functionality, Langmuir 1 (1985) 725–740, https://doi.org/10.1021/LA00066A016/ASSET/LA00066A016.FP.PNG_V03.
[76] T.G. Bee, E.M. Cross, A.J. Dias, et al., Control of wettability of polymers using organic surface chemistry, J. Adhes. Sci. Technol. 6 (1992) 719–731, https://doi.org/10.1163/156856192X01060.
[77] Ş. Berk, S. Kaya, E.K. Akkol, H. Bardakçı, A comprehensive and current review on the role of flavonoids in lung cancer–experimental and theoretical approaches, Phytomedicine 98 (2022) 153938, https://doi.org/10.1016/J.PHYMED.2022.153938.
[78] P.C. Stair, The concept of Lewis acids and bases applied to surfaces, J. Am. Chem. Soc. 104 (1982) 4044–4052, https://doi.org/10.1021/JA00379A002/ASSET/JA00379A002.FP.PNG_V03.
[79] F.M. Fowkes, M.A. Mostafa, Acid-base interactions in polymer adsorption, Ind. Eng. Chem. Prod. Res. Dev. 17 (1978) 3–7, https://doi.org/10.1021/I360065A002/ASSET/I360065A002.FP.PNG_V03.
[80] B. Shin, J. Shin, Y. Chandra Wirasembada, et al., Modeling the flux of volatile fatty acid in a membrane distillation with the effect of pH, J. Memb. Sci. 690 (2024) 122230, https://doi.org/10.1016/J.MEMSCI.2023.122230.
[81] M. Ferby, Z. He, Recovery of both volatile fatty acids and ammonium from simulated wastewater: Performance of membrane contactor and understanding the effects of osmotic distillation, J. Environ. Chem. Eng. 12 (2024) 113760, https://doi.org/10.1016/J.JECE.2024.113760.
[82] M. Qasim, I.U. Samad, N.A. Darwish, N. Hilal, Comprehensive review of membrane design and synthesis for membrane distillation, Desalination 518 (2021) 115168, https://doi.org/10.1016/J.DESAL.2021.115168.
[83] A. Samadi, T. Ni, E. Fontananova, et al., Engineering antiwetting hydrophobic surfaces for membrane distillation: A review, Desalination 563 (2023) 116722, https://doi.org/10.1016/J.DESAL.2023.116722.
[84] A. Gugliuzza, F. Ricca, E. Drioli, Controlled pore size, thickness and surface free energy of super-hydrophobic PVDF® and Hyflon®AD membranes, Desalination 200 (2006) 26–28, https://doi.org/10.1016/J.DESAL.2006.03.229.
[85] A. Razmjou, E. Arifin, G. Dong, et al., Superhydrophobic modification of TiO2 nanocomposite PVDF membranes for applications in membrane distillation, J. Memb. Sci. 415–416 (2012) 850–863, https://doi.org/10.1016/J.MEMSCI.2012.06.004.
[86] L.F. Ren, F. Xia, V. Chen, et al., TiO2-FTCS modified superhydrophobic PVDF electrospun nanofibrous membrane for desalination by direct contact membrane distillation, Desalination 423 (2017) 1–11, https://doi.org/10.1016/J.DESAL.2017.09.004.
[87] A. Al-Rumaihi, G. Mckay, H.R. Mackey, T. Al-Ansari, Environmental impact assessment of food waste management using two composting techniques. https://doi.org/10.3390/su12041595.
[88] P. Roy, A.K. Mohanty, P. Dick, M. Misra, A review on the challenges and choices for food waste valorization: Environmental and economic impacts, ACS Environ. Au 3 (2023) 58–75, https://doi.org/10.1021/ACSENVIRONAU.2C00050/ASSET/IMAGES/LARGE/VG2C00050_0005.JPEG.
[89] A. Siddiqua, J.N. Hahladakis, W.A.K.A. Al-Attiya, An overview of the environmental pollution and health effects associated with waste landfilling and open dumping, in: Environmental Science and Pollution Research, 2022, https://doi.org/10.1007/S11356-022-21578-Z.
[90] Global food losses and food waste. https://www.fao.org/4/mb060e/mb060e00.htm. Accessed 6 Aug 2024.
[91] P.R.J. Lukitawesa, R. Millati, et al., Factors influencing volatile fatty acids production from food wastes via anaerobic digestion, Bioengineered 11 (2020) 39–52, https://doi.org/10.1080/21655979.2019.1703544.
[92] A. Selvam, P.M.K. Ilamathi, M. Udayakumar, et al., . Food waste properties current developments in biotechnology and bioengineering, Sust. Food Waste Manage.: Resour. Recov. Treat. 11–41 (2021), https://doi.org/10.1016/B978-0-12-819148-4.00002-6.
[93] K. Luo, Y. Pang, Q. Yang, et al., A critical review of volatile fatty acids produced from waste activated sludge: Enhanced strategies and its applications, Env. Sci. Pollut. Res. 26 (14) (2019) 13984–13998, https://doi.org/10.1007/S11356-019-04798-8.